SAND2018-11540C

SolarPACES 2018
Solar Power & Chemical Energy Systems
October 2–5, 2018 | Casablanca, Morocco

Point-Focus Systems

A Review of Papers Presented at SolarPACES 2018

Clifford K. Ho and Julius E. Yellowhair
Sandia National Laboratories

Sandia National Laboratories

U.S. DEPARTMENT OF ENERGY

Sandia National Laboratories is a multimission laboratory managed and operated by National Technology and Engineering Solutions of Sandia, LLC, a wholly owned subsidiary of Honeywell International, Inc., for the U.S. Department of Energy's National Nuclear Security Administration under contract DE-NA0003525.

NNSA National Nuclear Security Administration

~120 Point-Focus Papers

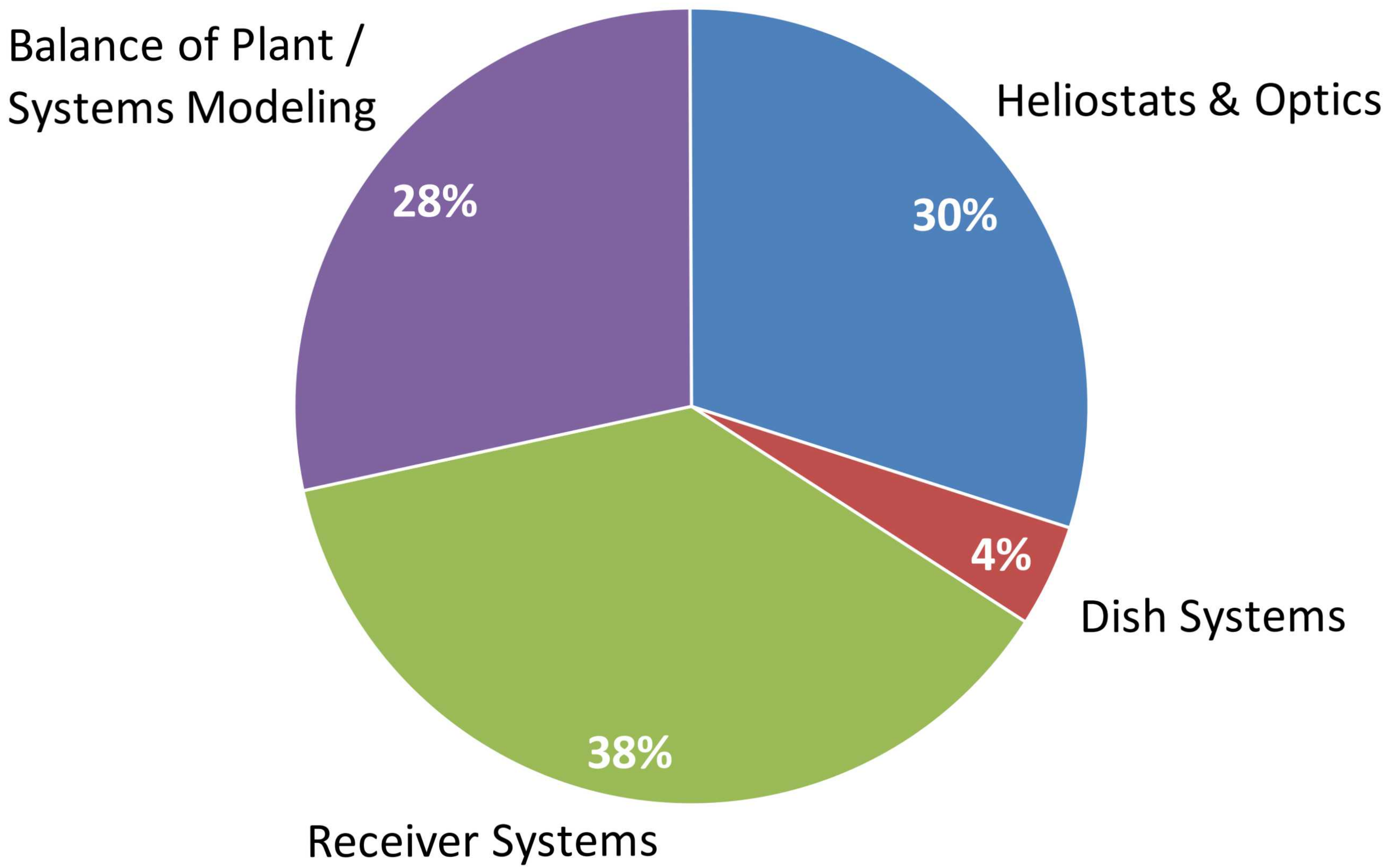

Point-Focus Papers by Country

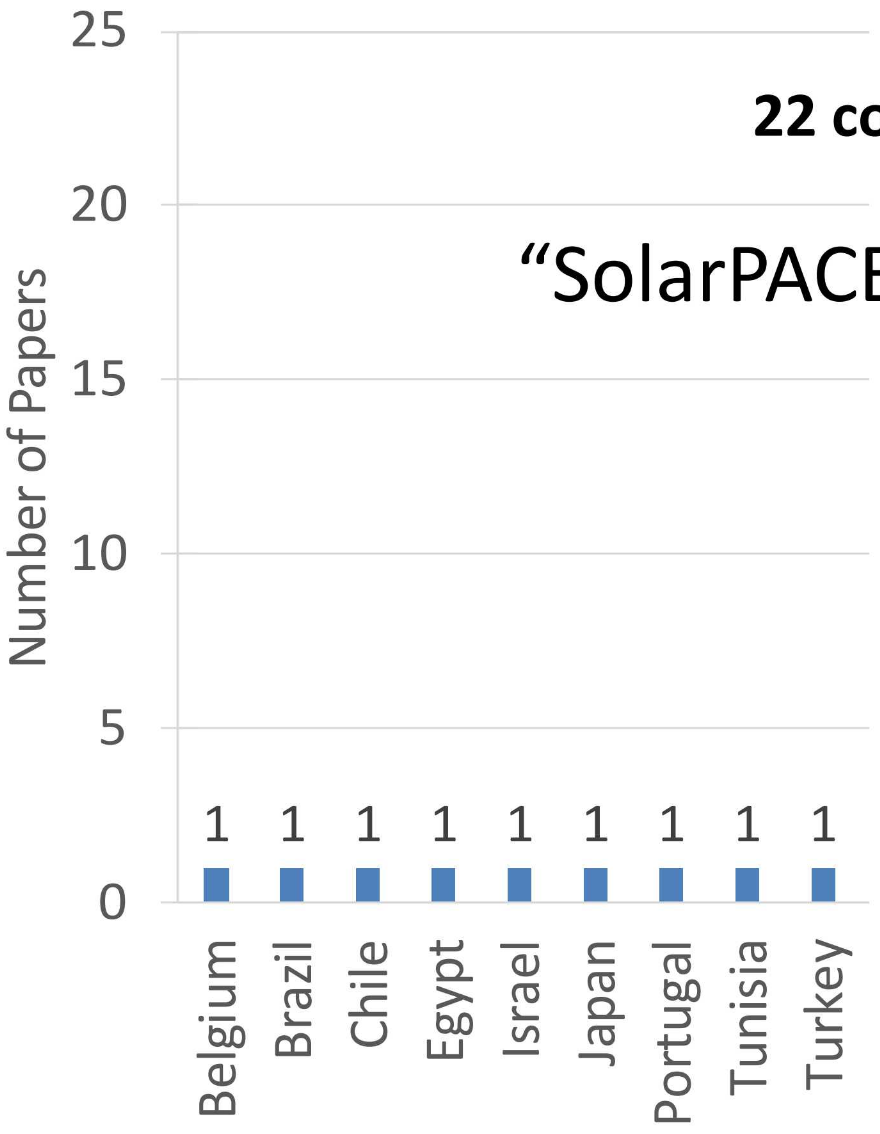

22 countries

"SolarPACES Olympics"

Point-Focus Papers by Country

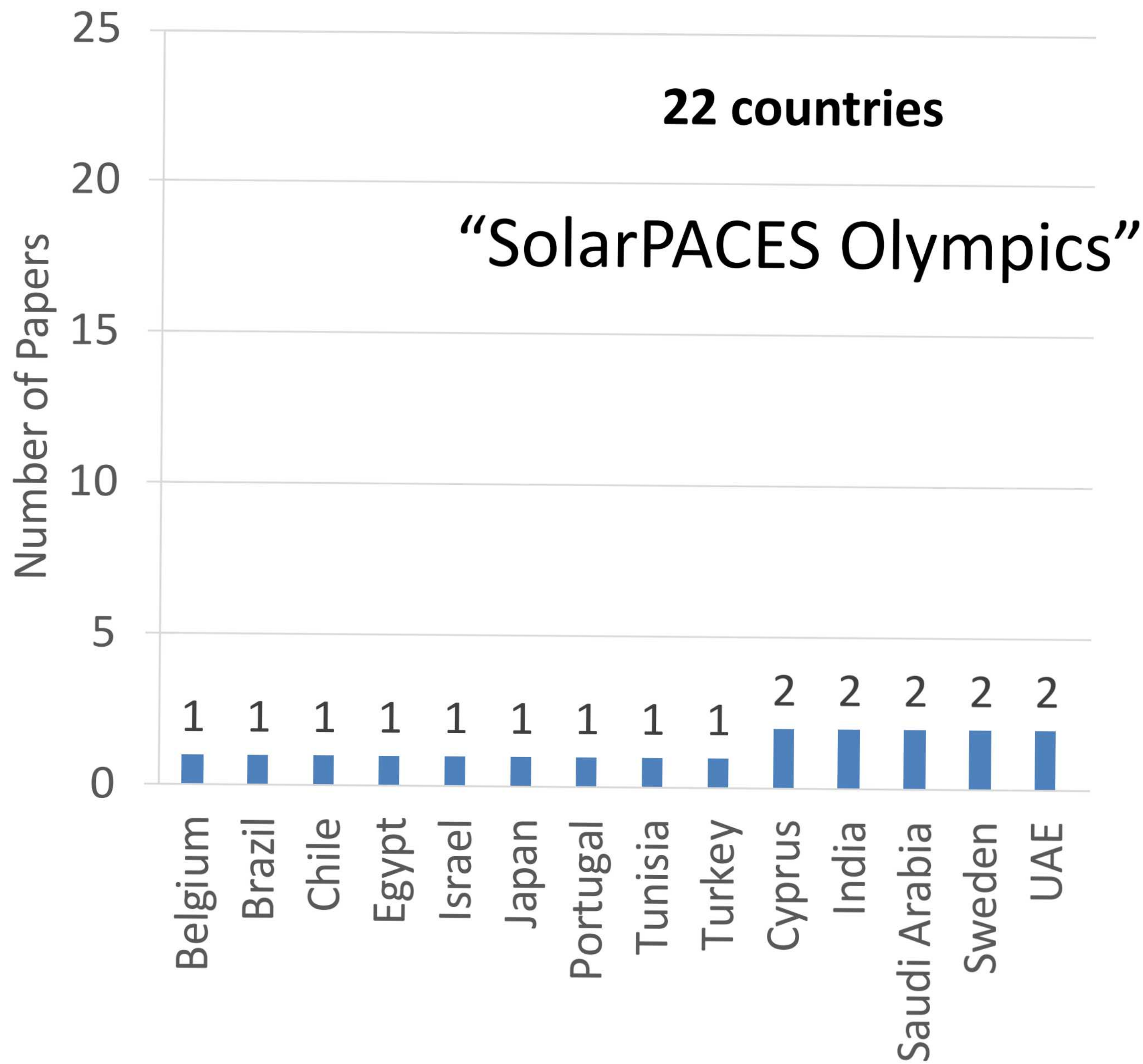

Point-Focus Papers by Country

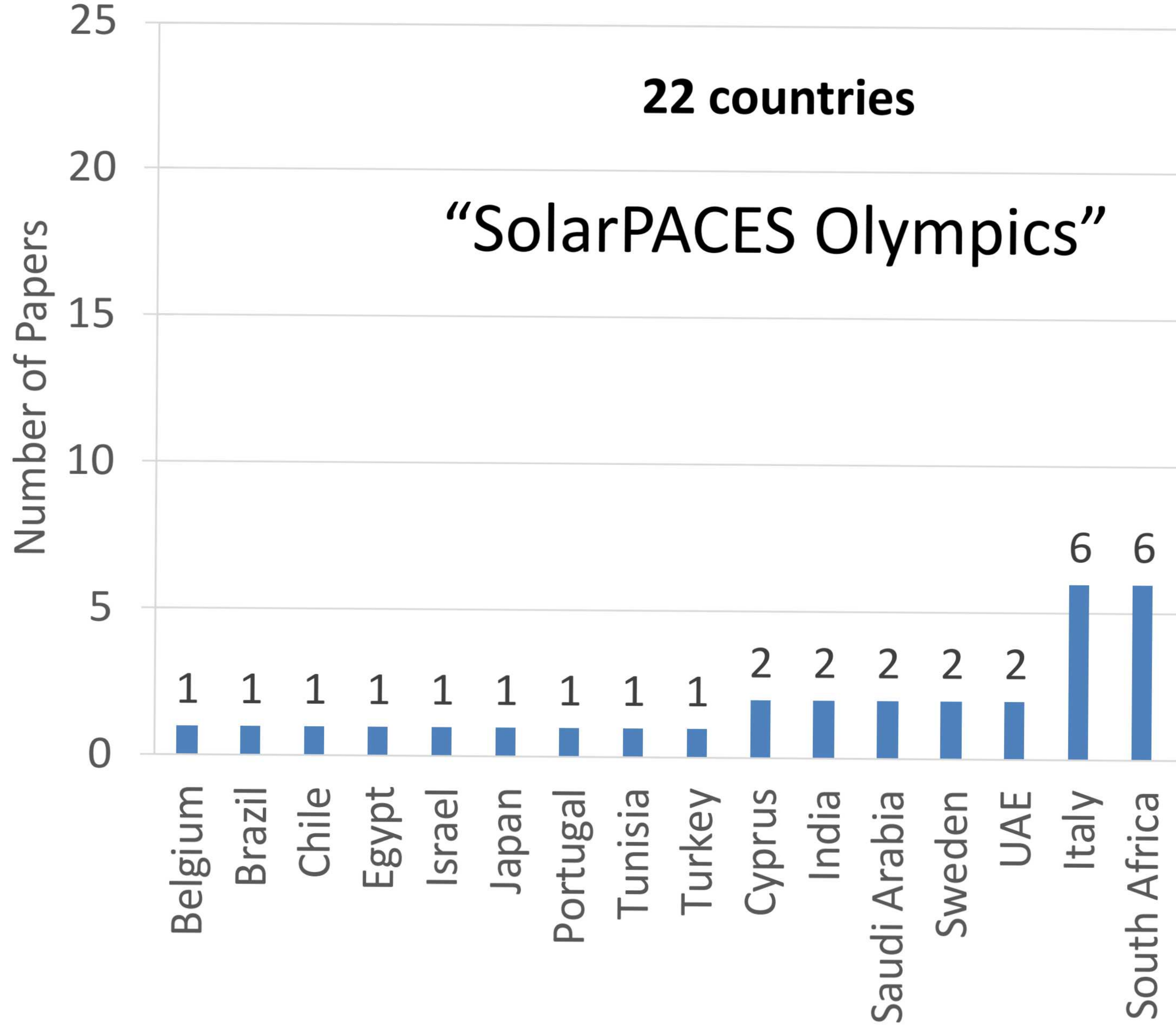

Point-Focus Papers by Country

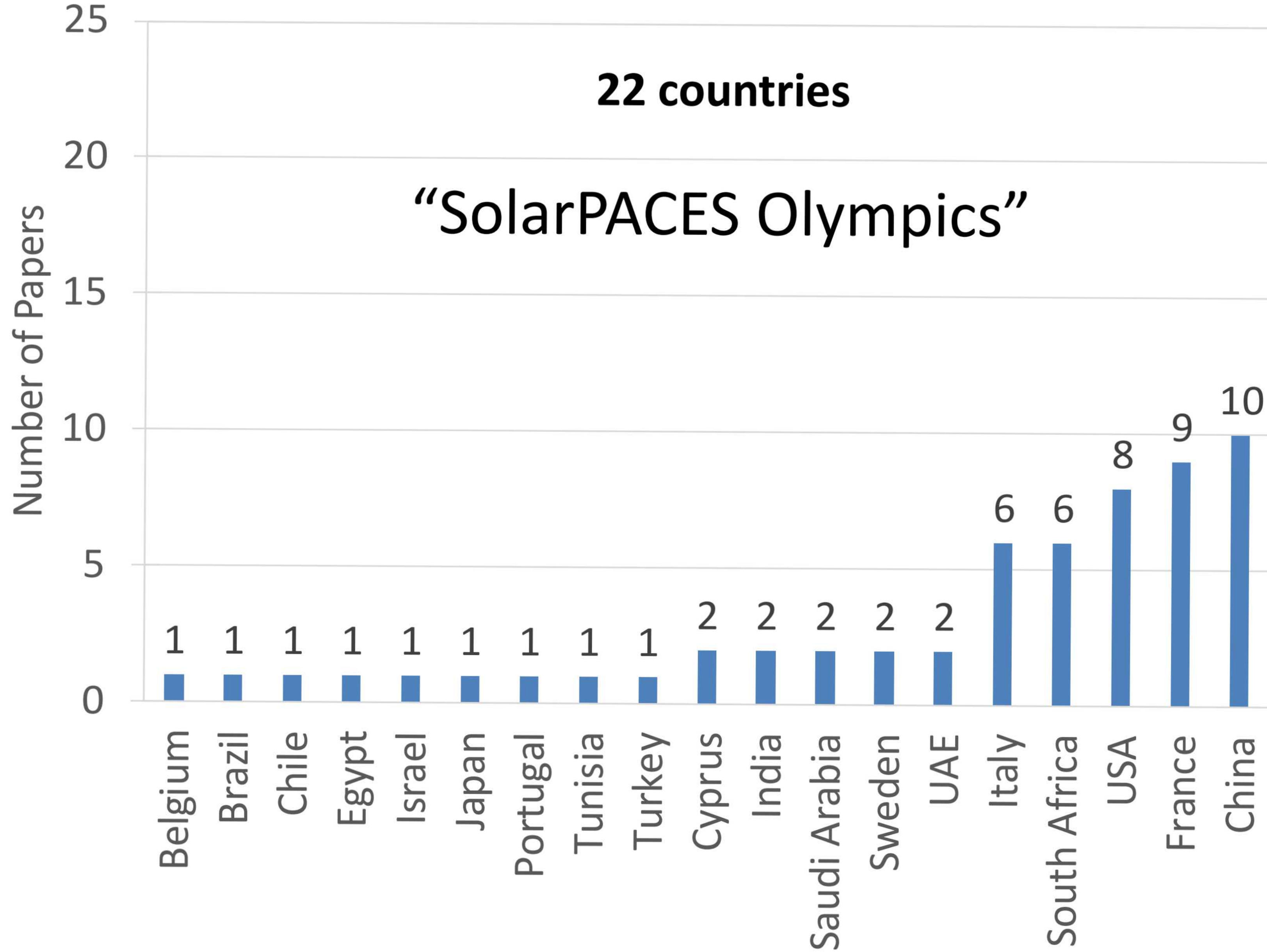

Point-Focus Papers by Country

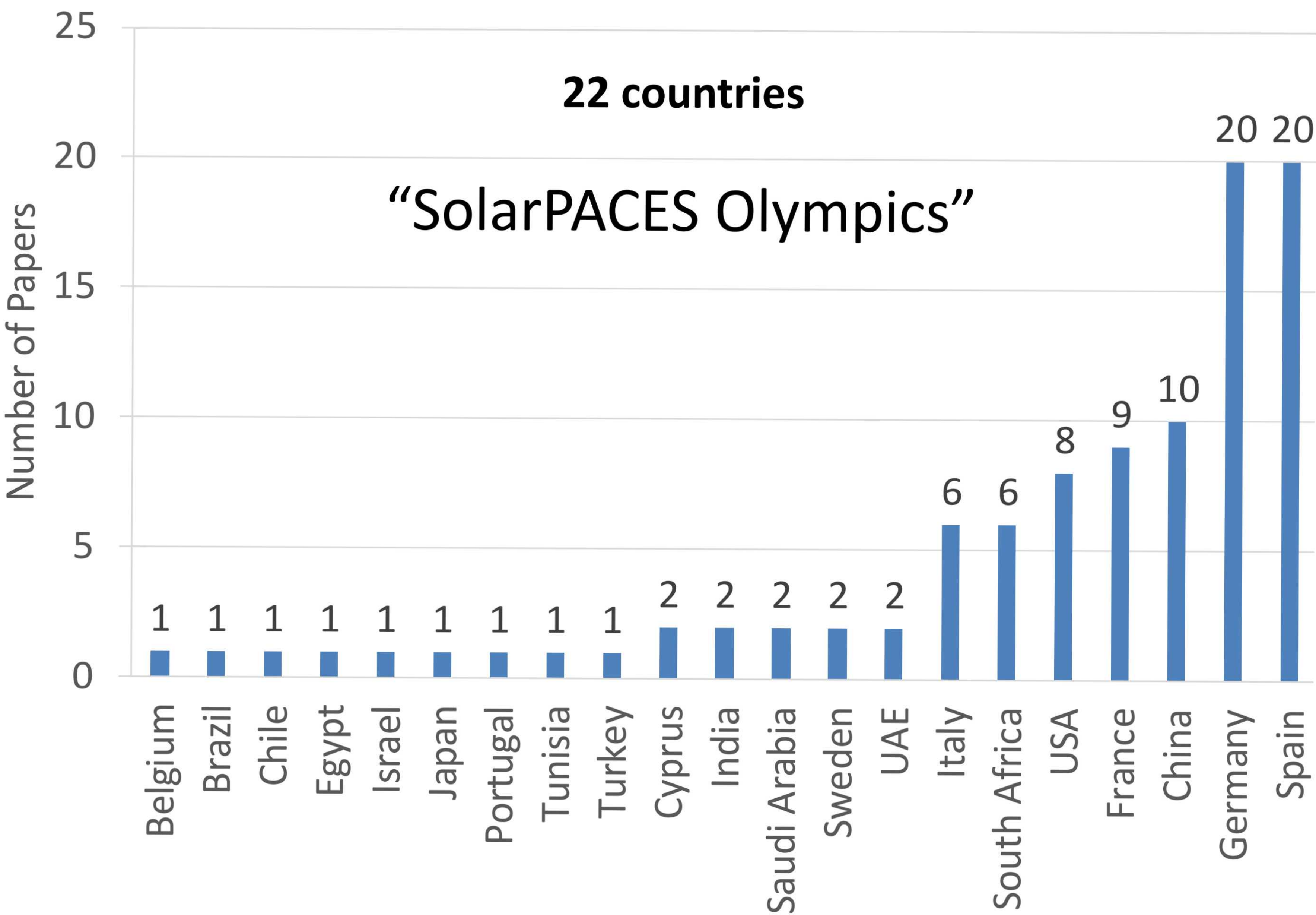

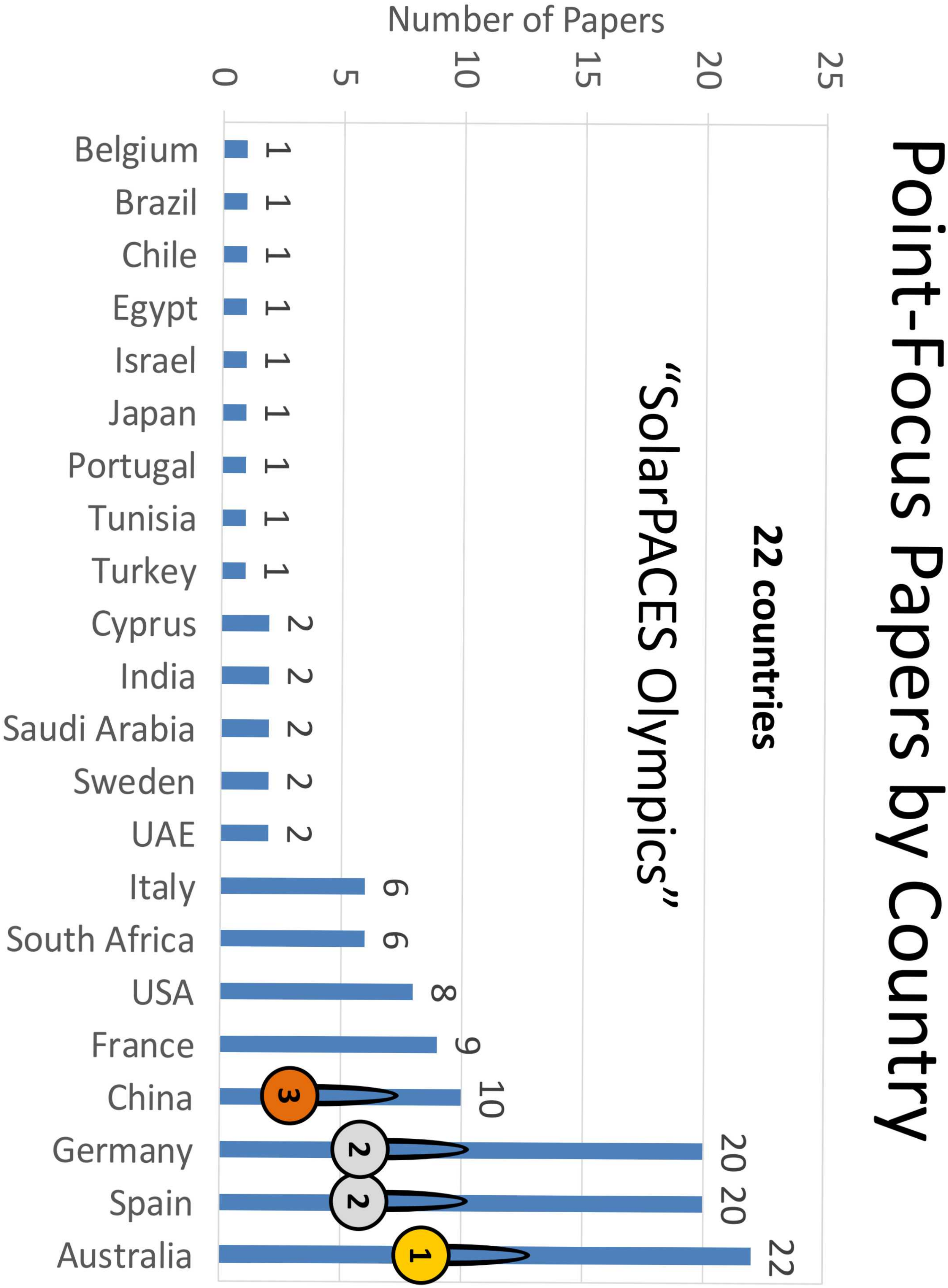

Point-Focus Papers by Country
22 countries
"SolarPACES Olympics"
Number of Papers
0
5
10
15
20
25
Belgium 1
Brazil 1
Chile 1
Egypt 1
Israel 1
Japan 1
Portugal 1
Tunisia 1
Turkey 1
Cyprus 2
India 2
Saudi Arabia 2
Sweden 2
UAE 2
Italy 6
South Africa 6
USA 8
France 9
China 10
Germany 20
Spain 20
Australia 22
3
2
2
1

Point-Focus Systems

- Heliostats, Dish Systems, and Optics
- Receivers
- Systems Modeling

Point-Focus Optics Trends

30 total papers

- 14 papers
- 16 posters

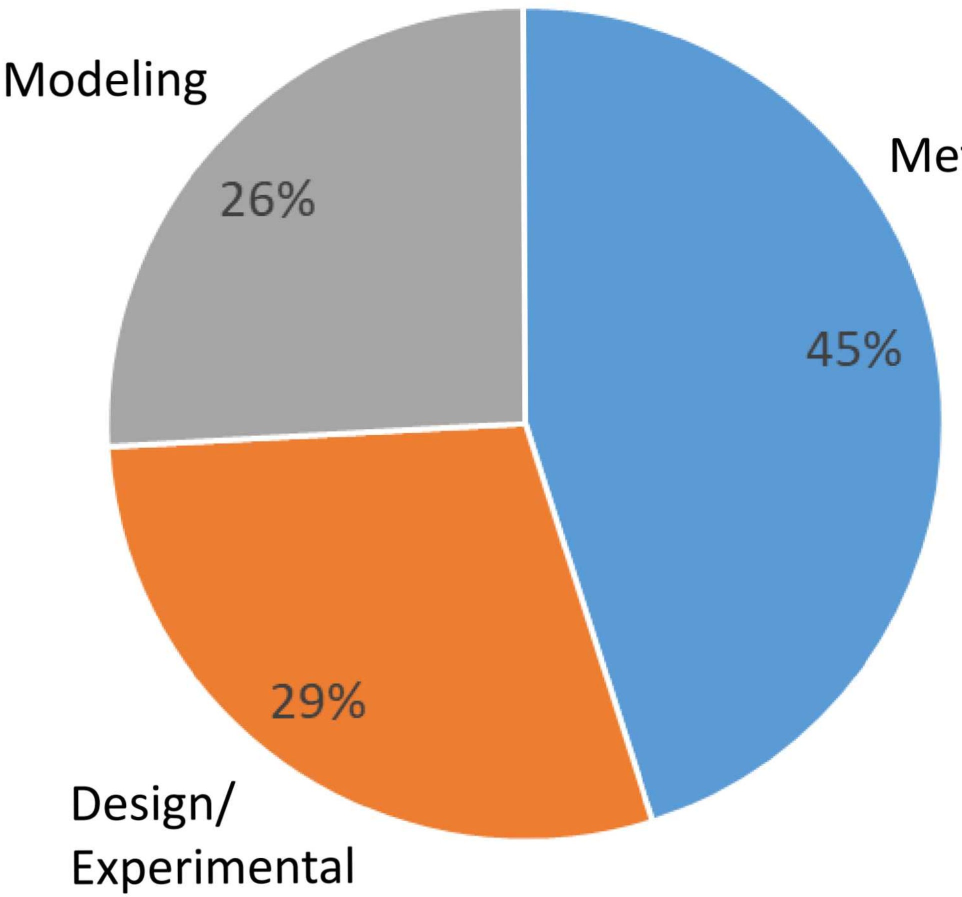

Metrology Papers

Optical Error Parameters

Slope Error	**Schedlar**, et al. **Niefer**, et al.; **Les**, et al;
Canting	**Andraka**; **Zhu**;
Tracking	**Collins**, et al.; **Guo**, et al.; **Les**, et al;
Reflectance/ Soiling	**Wang**; **Bonanos**, et al.;
Atmospheric Attenuation	**Sanchez**, et al.;

AIMFAST for Heliostats: Canting Tool for Long Focal Lengths

(Andraka)

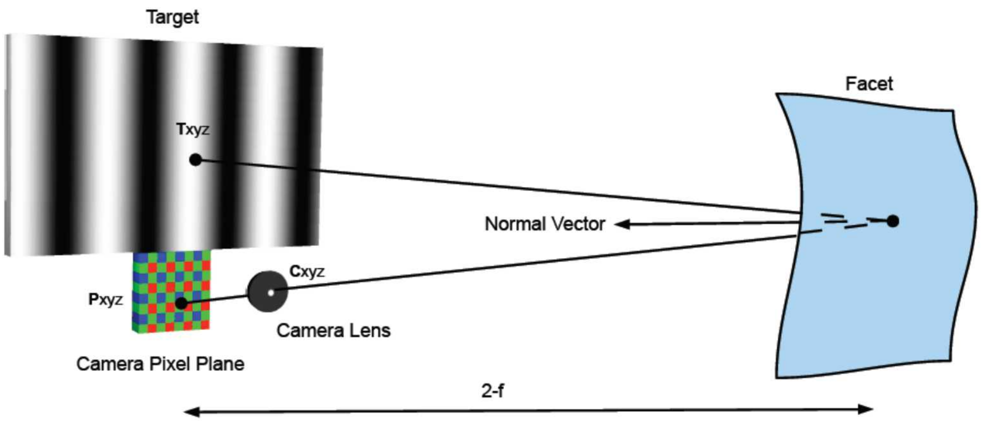

Figure 1. Single-facet test stand (left) and 24-facet lab-scale heliostat after initial alignment (right).

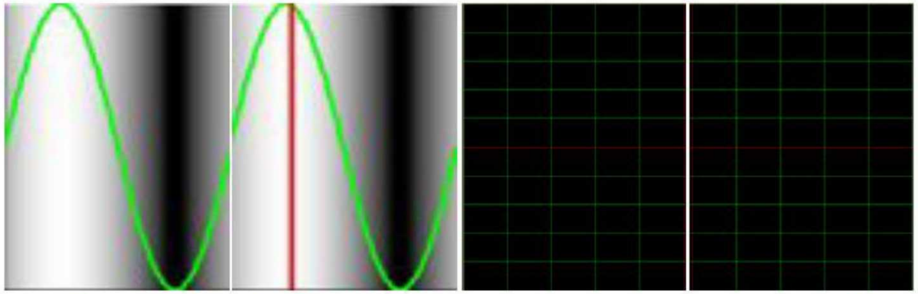

Figure 2. Two-projector target. Left, fringe patter extends across two projector images smoothly by using a single Windows figure. Right, the grid line in the characterization grid is doubled at the discontinuity, shown in red.

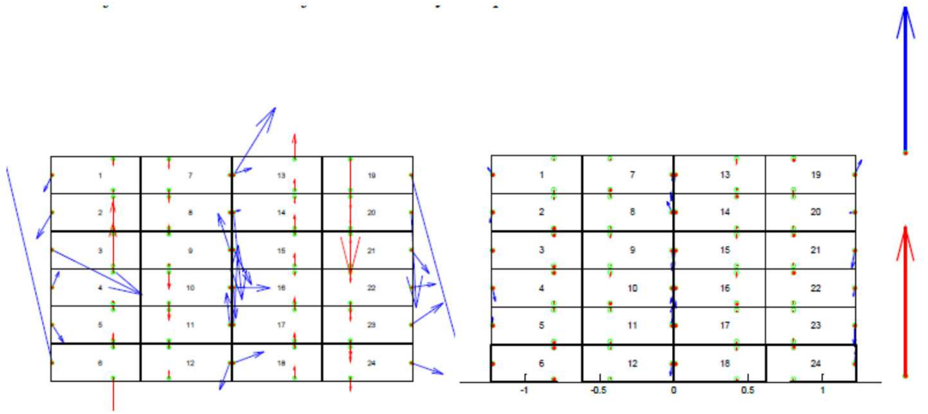

Figure 8. 24-Facet Lab Heliostat before and after final alignment. Facet 6 adjustment screws could not be adjusted due to severe galling. The blue vectors represent total canting error of each facet, while the red vectors indicate the adjustment needed at each screw. The red reference arrow is 1mm of adjustment, while the blue is 1 mrad of total canting error. Facet 6 is excluded from the right hand image.

Heliostat Testing According of SolarPACES Task 3 Guideline

(Nieffer, et al.)

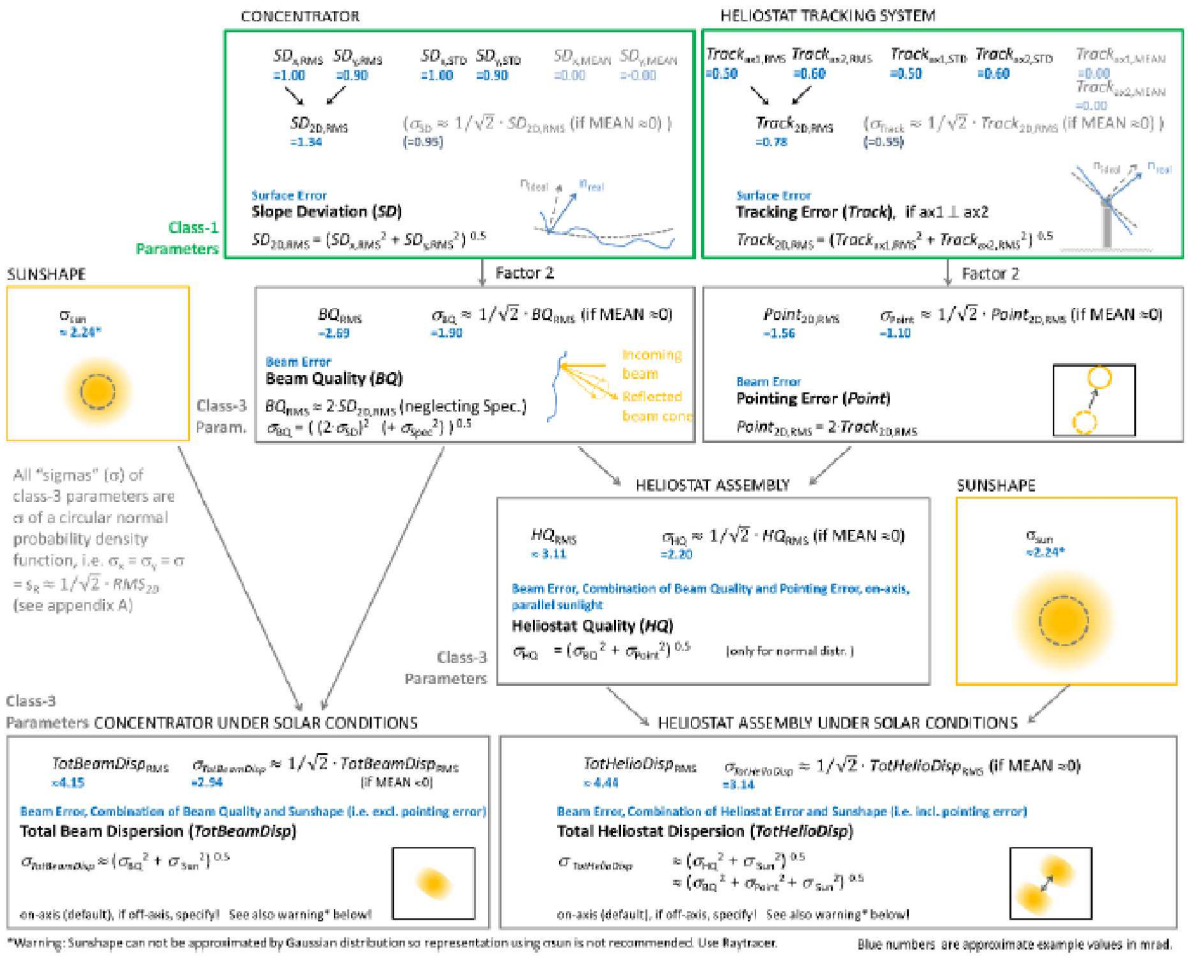

FIGURE 0-1: Convolution of optical errors from one-dimensional surface or tracking errors to the total heliostat error with exemplary values in blue [1]

Solar Field Heliostat Selection Based on Polygon Optimization

(Schöttl, et al.)

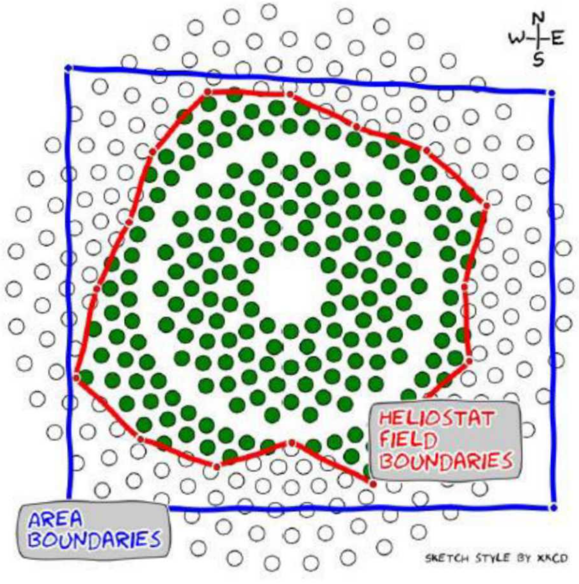

FIGURE 1. Sketch qualitatively describing the optimization problem. Area boundaries are blue, heliostat field boundaries are red, non-selected heliostats are white circles, selected heliostats are green circles.

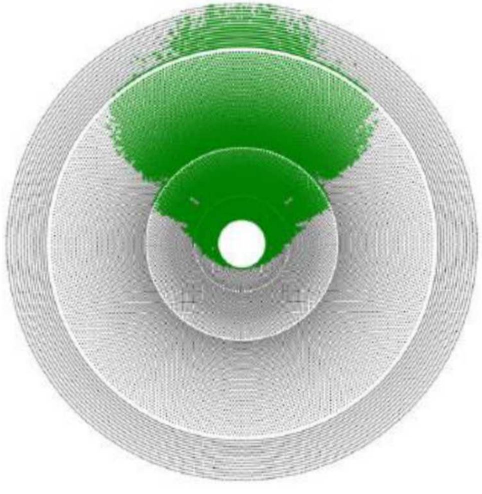

b) Case A

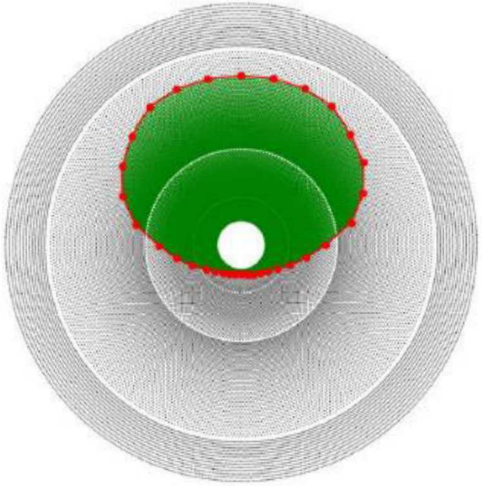

d) Case C

Point-Focus Systems

- Collectors and Optics
- Receivers
- Systems Modeling

Trends in Receivers

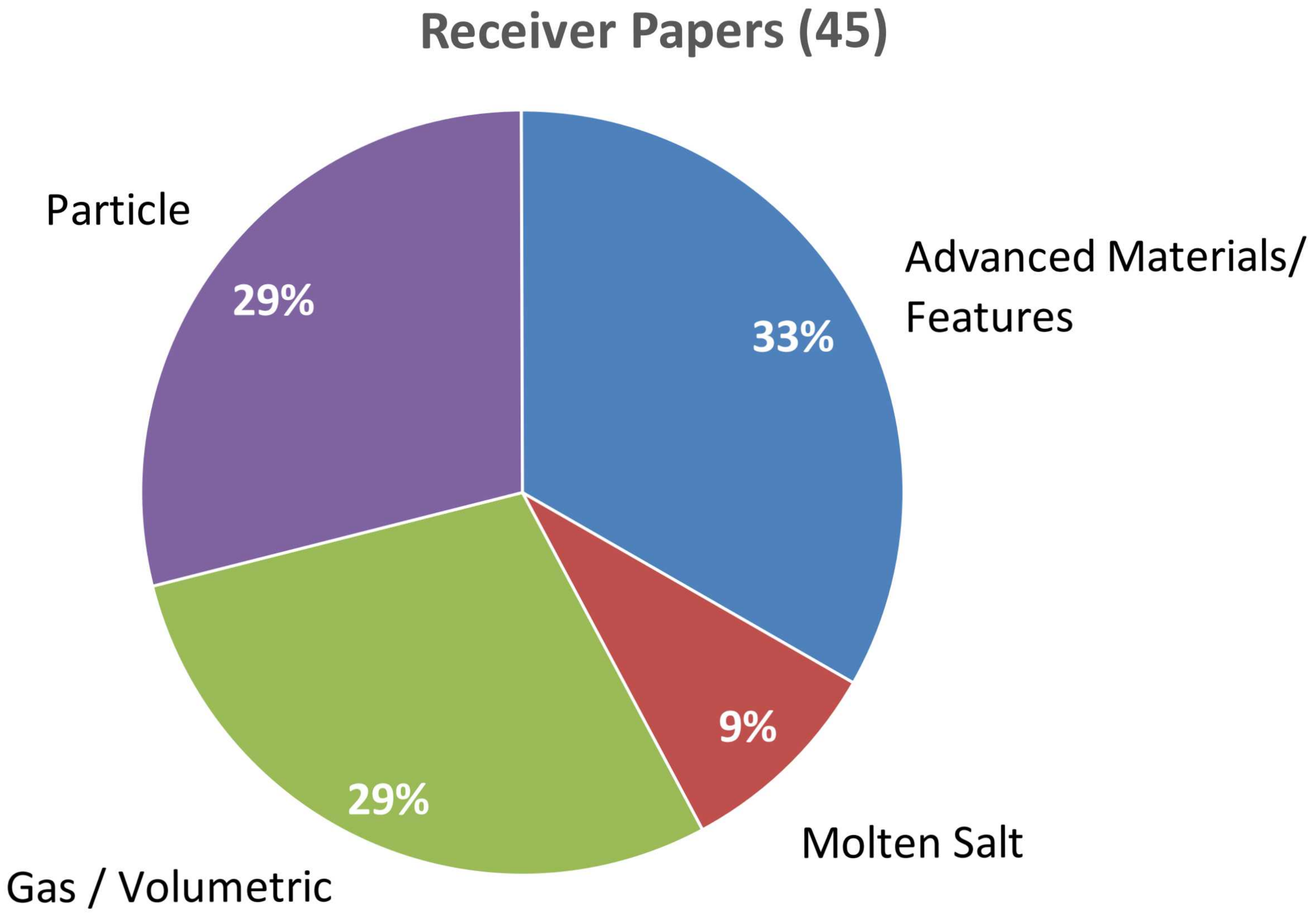

Receiver Papers

- Molten Salt

- Gas / Volumetric

- Particles

- Advanced Materials / Features

Using Corrugated Tubes in External Molten Salt Receivers

(Uhlig et al., DLR)

FIGURE 6. Helical ribs witch variable pitch and groove depth along tube length

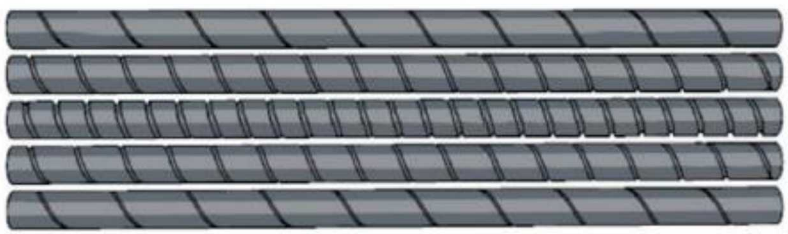

FIGURE 7. Tailored receiver panel using different geometry of corrugated tubes

FIGURE 8. Partial helical ribs

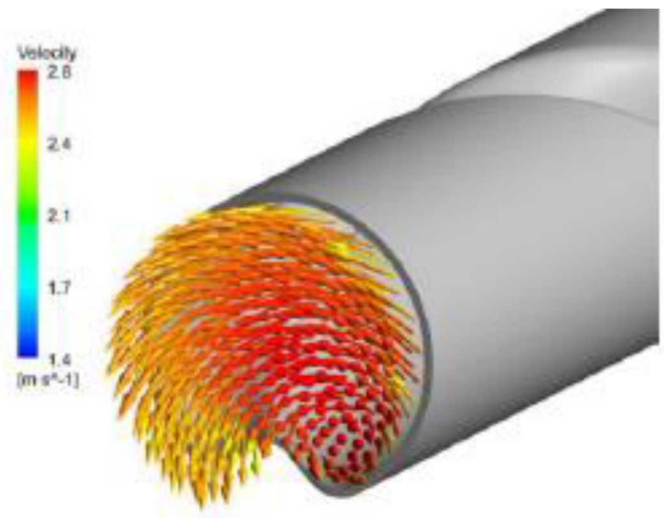

CFD simulations sowed that helical ribs can induce internal mixing of molten salt to reduce film temperature and enable higher fluxes and outlet temperatures. Need to balance, flux, flow rate, and temperatures.

Effect of eccentricity on the thermal stresses in a bayonet tube for solar power tower receivers

(Alvarez et al., University Carlos III of Madrid)

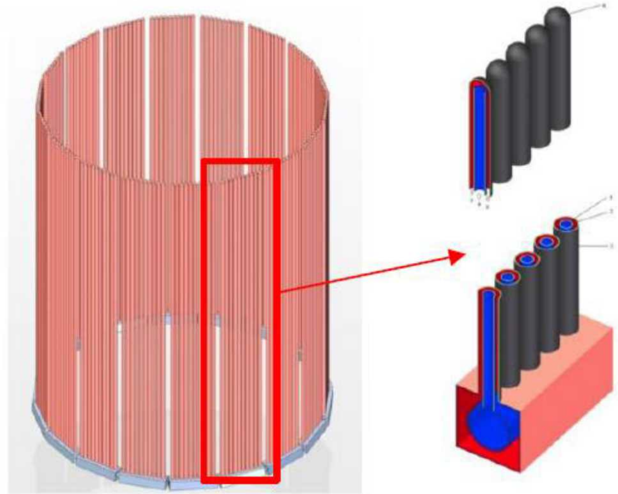

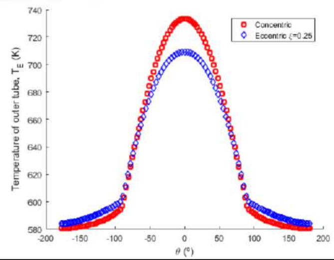

Bayonet tubes with concentric flow: eccentric shape reduces peak temperatures and stresses on irradiated tube.

Central Receiver Heat Transfer Enhancement Using Jet Impingement with Passive Velocity Excitation

(Craig, University of Pretoria

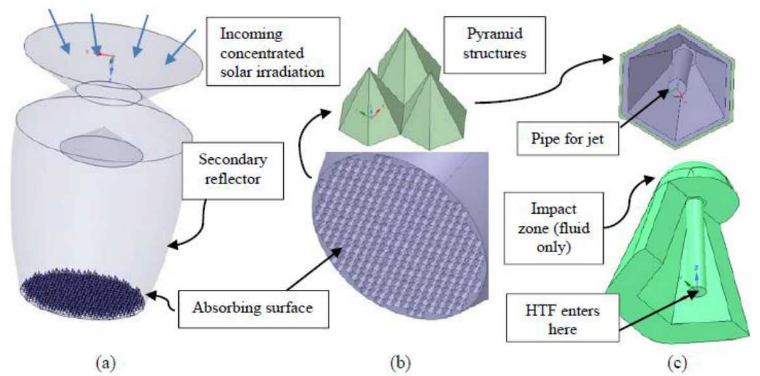

GURE 1. Proposed central cavity receiver (Craig et al [5]): a) absorber surface and secondary reflective surfaces, b) pyramid array structure, c) internal geometry with jet pipe and impact zone

Light-trapping features with internal impinging flows and passive flow perturbation to increase heat transfer. Need to balance with increase in pressure drop.

Direct Absorption Volumetric Molten Salt Solar Receiver/Thermal Energy Storage System and Floating Modular Transparent Cover

(Calvet et al., MASDAR Institute, Khalifa University
Lahlou et al., MASDAR Institute, Khalifa University)

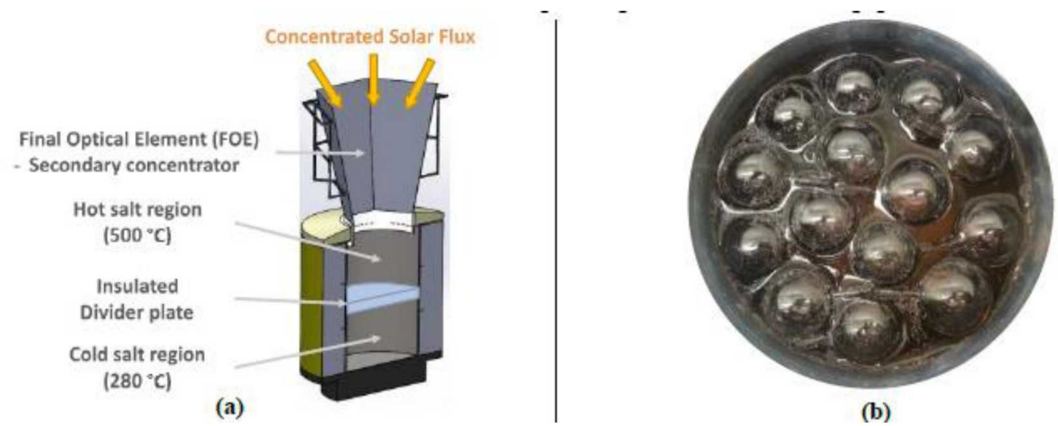

Direct beam-down molten-salt volumetric absorption tests showed uniform heating at ~475 C. Floating fused-silica spheres reduced salt and heat losses in bench-scale tests.

Corrosion monitoring of ferritic-martensitic steels in molten salt environments for CSP applications

(Perez et al., University of Madrid)

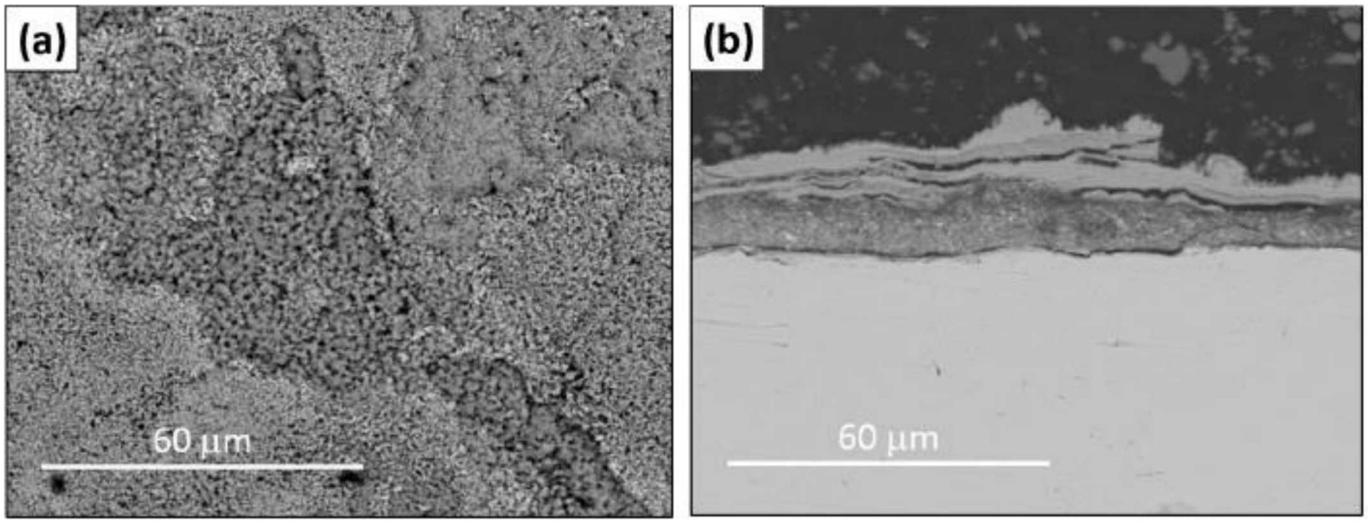

Fig. 3: SEM micrographs of P91 after 1000 h of testing: (a) superficial aspect; (b) cross-section.

Real-time electrochemical impedance spectroscopy demonstrated for diffusion controlled porous-layer corrosion of P91 by molten salt and confirmed by SEM and XRD.

Receiver Papers

- Molten Salt
- Gas / Volumetric
- Particles
- Advanced Materials / Features

Design and testing of externally finned tube cavity receiver for Brayton cycle preheating purposes

(Basson et al., Stellenbosch University)

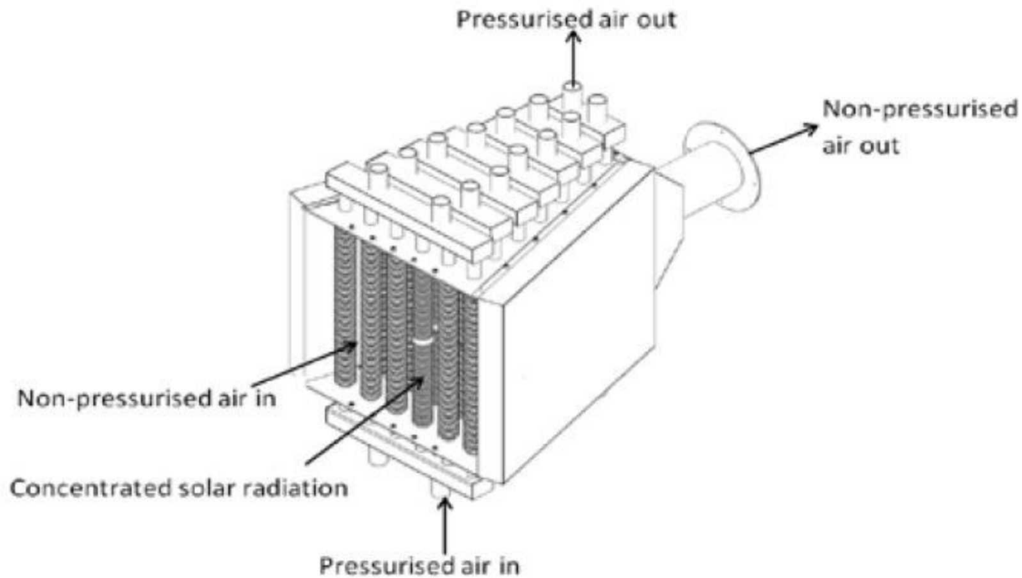

Finned external tubes in a cavity receiver intended to provide radiative trapping and reduced convective losses in a hybrid air receiver. Modelling shows mixed results.

Experimental and numerical evaluation of a small array of ceramic foam volumetric absorbers

(Zaversky et al., CENER, CIEMAT, Franhofer IKTS)

Modular sintered SiC foam with optimized cell density and porosity, and frustum shape to homogenize air speed, have achieved 900 C.

Performance Assessment of an Improved Open Volumetric Receiver Design with 240 MWth

(Stadler et al., DLR)

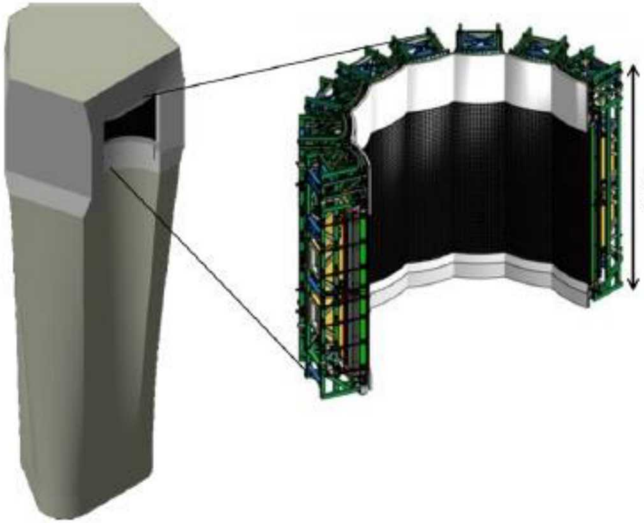

A novel receiver design for a 240 MWth solar tower was optimized for reduced radiative losses and high air return ratios.

Experimental study of a heat pipe pressurized air receiver

(Bai et al., Chines Academy of Sciences)

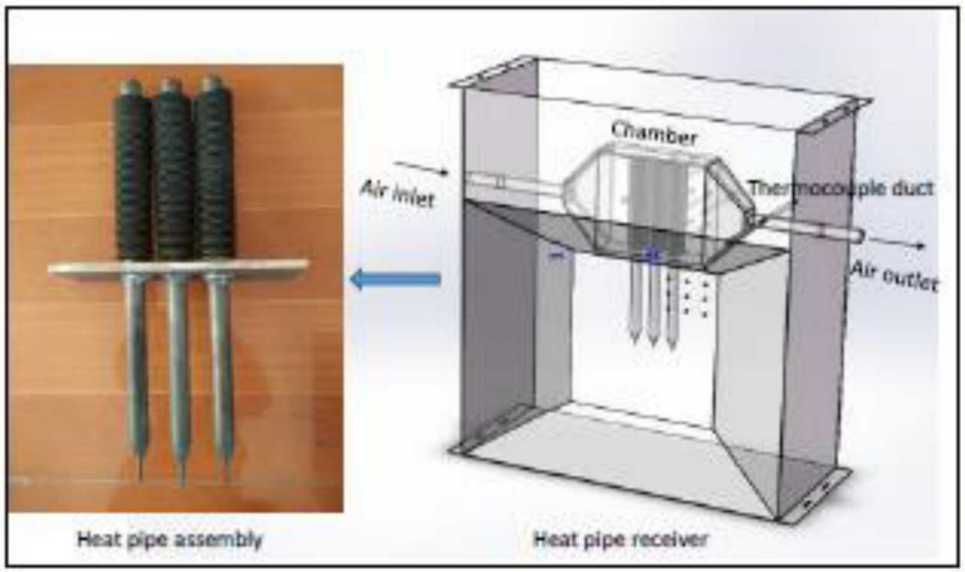

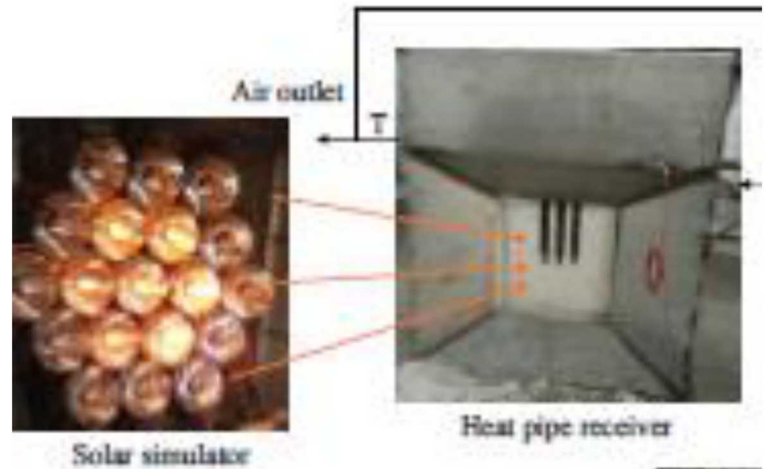

Heat pipes tested to heat pressurized air for solar hybrid gas-turbine system. Achieved air temperature of ~620 C with ~80% efficiency.

Receiver Papers

- Molten Salt
- Gas / Volumetric
- Particles
- Advanced Materials / Features

Numerical and experimental investigation of a novel multi-stage falling particle receiver

(Kim et al., CSIRO)

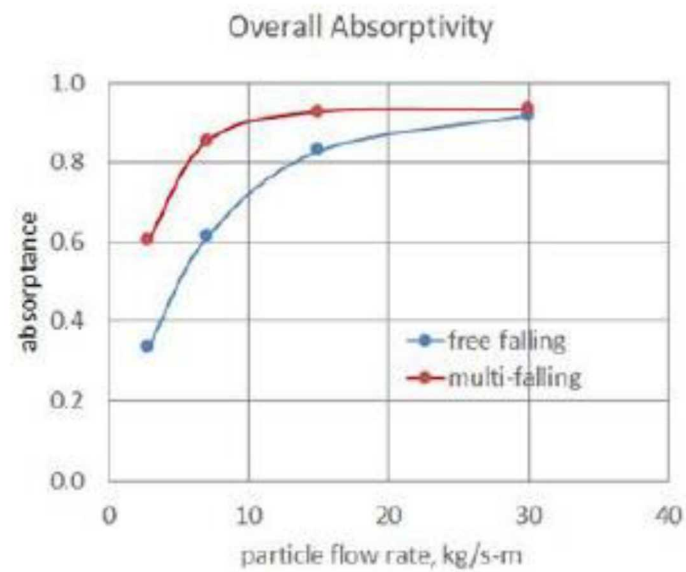

Simulations and testing of multi-stage catch-and-release particle receiver showed increase in opacity and solar absorptance relative to free-fall.

On-Sun Particle Receiver Testing, Simulation, and Mass Flow Control

(Ho et al., Sandia National Laboratories
Mills and Ho, Sandia National Laboratories)

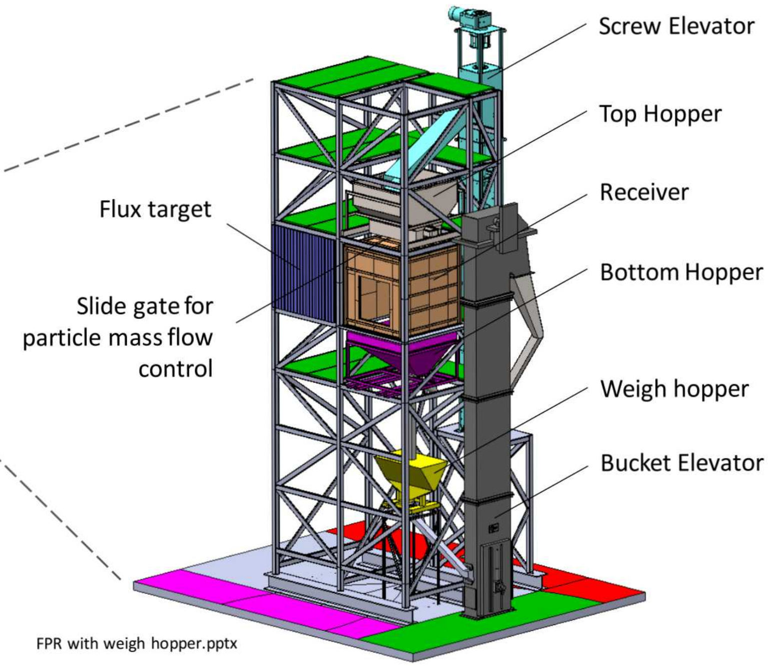

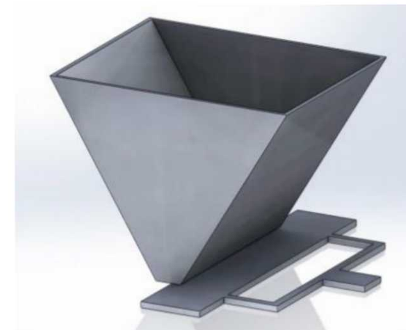

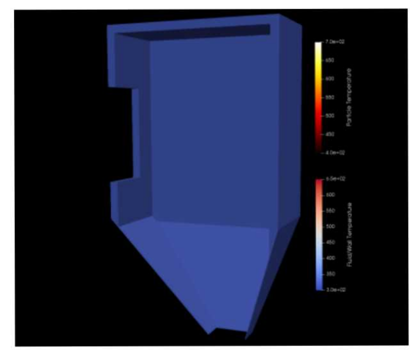

~1 MW_t on-sun particle receiver tests demonstrated automated particle temperature and mass flow control with high temperatures (~700 C) and efficiencies of ~80%. Simulations showed significant impacts of wind and convective heat losses.

Operational Experience of a Centrifugal Particle Receiver Prototype

(Ebert et al., DLR)

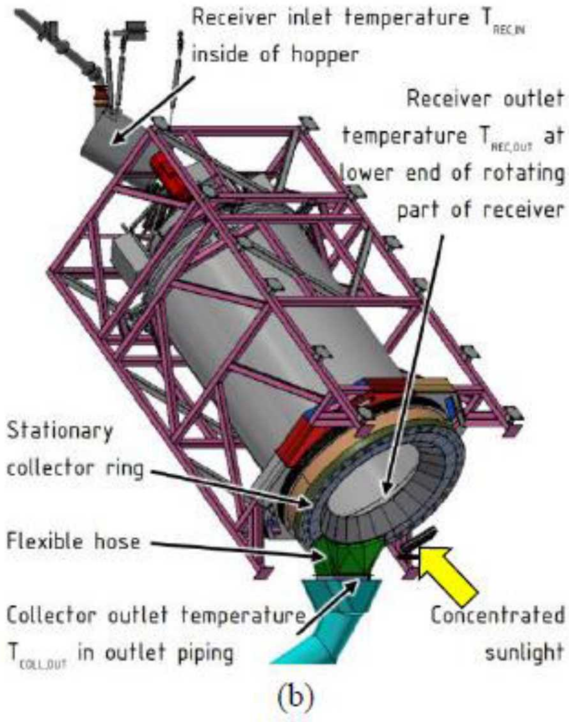

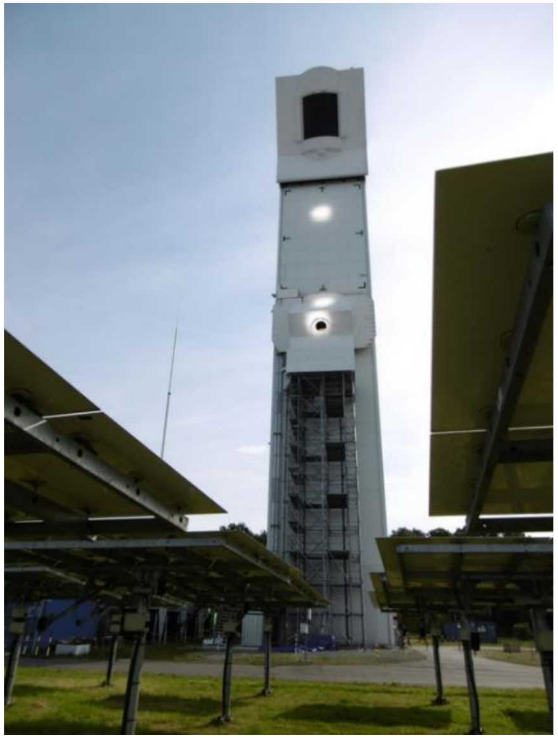

On-sun tests achieved ~965 C average particle outlet temperature. Lessons learned include ways to improve particle flow behavior and reduce particle loss through aperture.

Experimental Study on Thermal Performance of a Novel Solar Particle Receiver

(Xie et al., Zhejiang University)

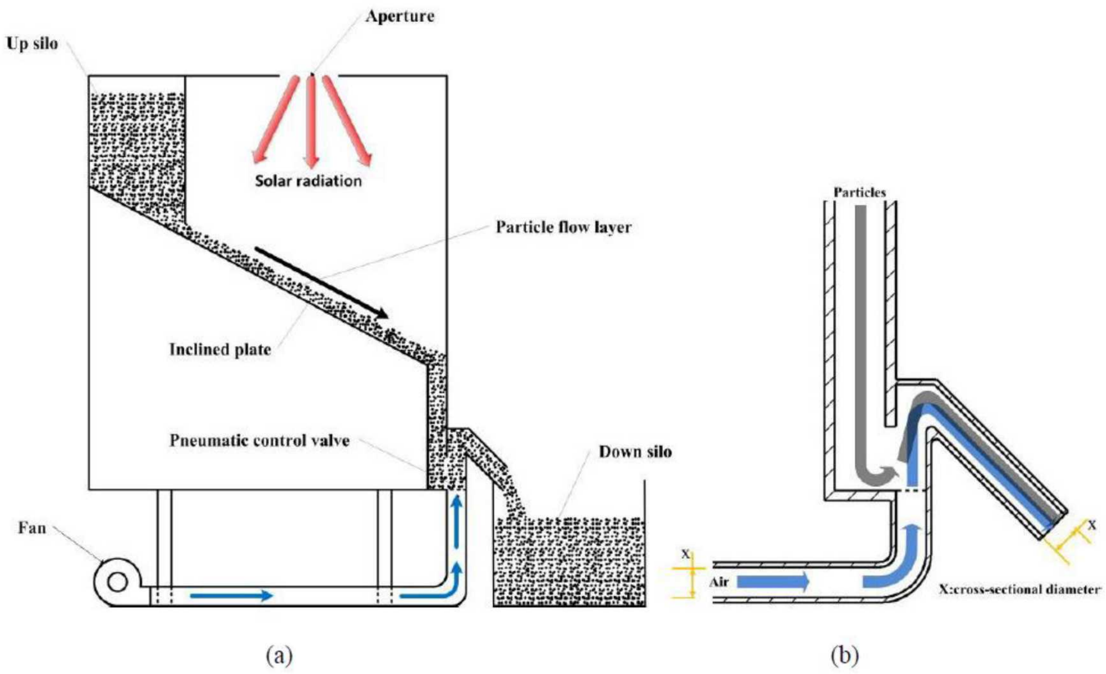

Fig. 1: Schematic of particle receiver (a) and pneumatic control valve (b).

Particles flowing down an inclined surface are irradiated from a beam-down system with flow control from a pneumatic valve. Preliminary tests achieved 500 C at 60% efficiency.

Receiver Papers

- Molten Salt
- Gas / Volumetric
- Particles
- Advanced Materials / Features

Accelerated aging and characterisation of a novel absorber coating on Inconel 625 and SS316L substrates for high-temperature applications

(Tsuda et al., Nano Frontier Technology and ANU)

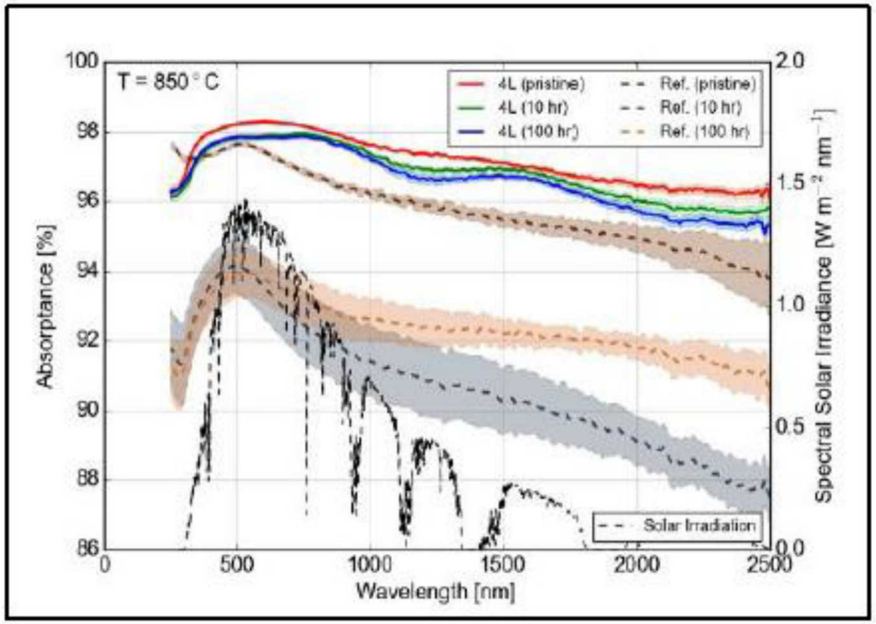

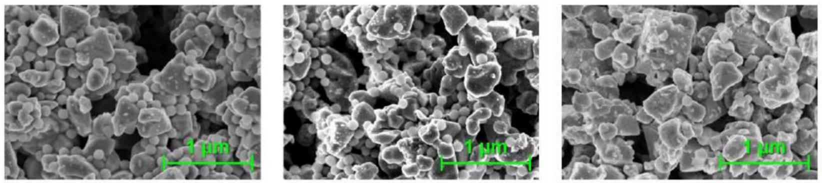

(a) pristine state (b) after 10 hours (c) after 100 hours

Micro-textured multi-layer coating of TiO_2 and black pigments showed superior absorptance (97%) and aging relative to Pyromark 2500, which decreased from ~96% to ~92% after 100 hrs at 850 C.

Bladed Receivers

- Convective heat loss from a bladed solar receiver, Torres et al., ANU
- Optical and Radiation Considerations in Bladed Receiver Designs for Central Tower Systems, Ye et al., ANU
- Towards testing of a second-generation bladed receiver, Pye et al., ANU

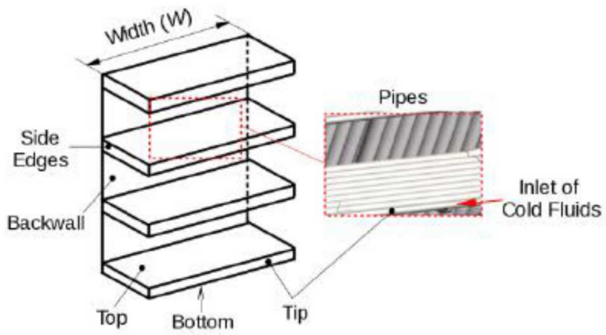

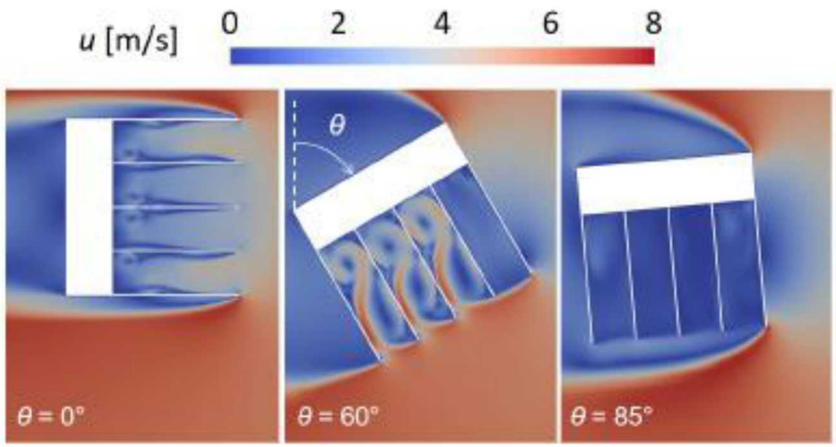

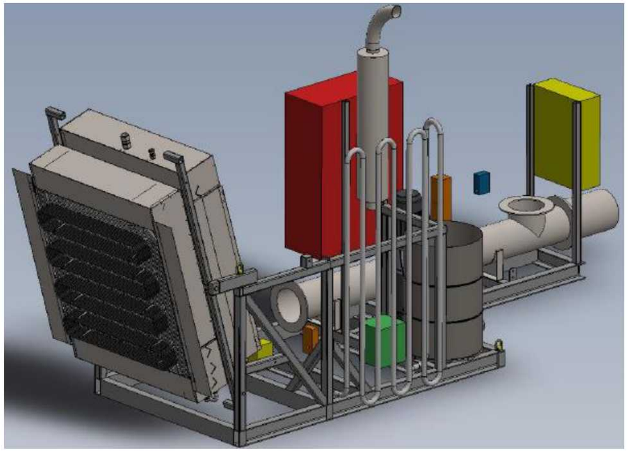

Bladed receivers were studied numerically and experimentally to optimize solar collection, minimize thermal losses, and perform technoeconomic analyses. On-sun test is being prepared.

Novel Low-Cost Quartz Window for Reducing Heat Losses in Concentrating Solar Power Applications

(Sullivan and Kesseli, Brayton Energy)

Figure 1 – Quartz-tube window mounted over a 250 kW_{th} cavity receiver aperature

Quartz tubes placed in aperture of cavity receiver reduced heat losses by 9 – 36%, despite reflective losses.

Heliostat Aiming Strategies for Novel Receiver Designs

Aiming Point Optimization for Advanced Tubular Receiver Designs

(Frantz and Flesch, DLR)

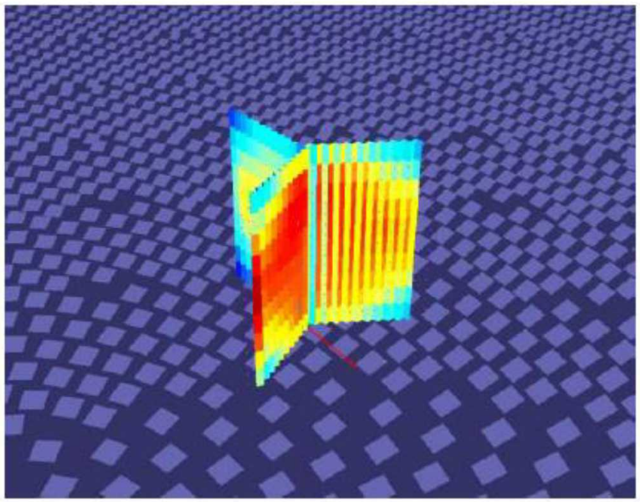

Aiming strategy developed for novel STAR panel arrangement that allows for increase in optical receiver efficiency

Aiming Strategy on the Next-CSP Receiver: Coupling of TABU Search, Ray-Tracing Software Solstice and Thermal Model

(Grange et al., PROMES-CRNS)

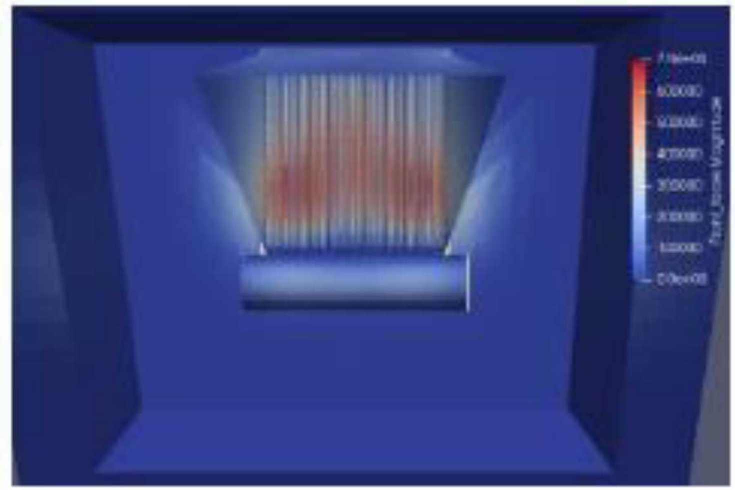

Aiming strategy developed for novel dense-suspension particle receiver that increased uniformity of flux distribution but reduced particle temperatures.

Point-Focus Systems

- Collectors and Optics
- Receivers
- Systems Modeling

Multi Tower Systems and Simulation Tools

Arbes et al., SBP

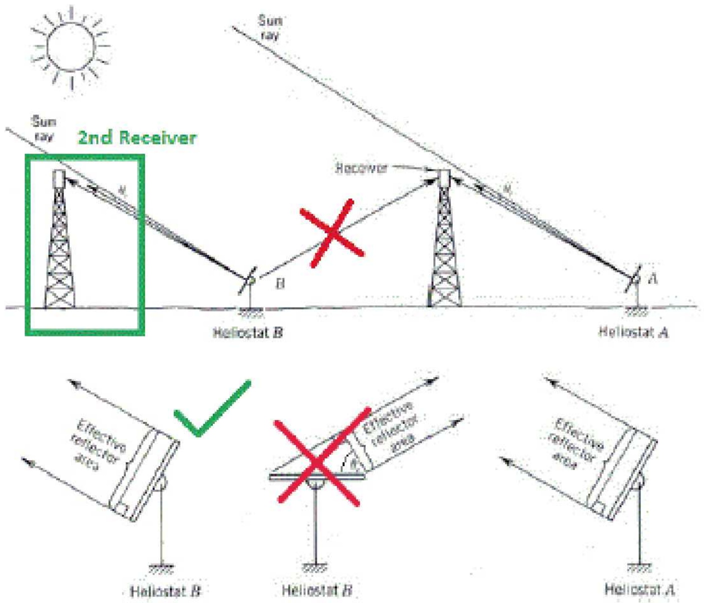

FIGURE 1: Improving a heliostats cosine efficiency

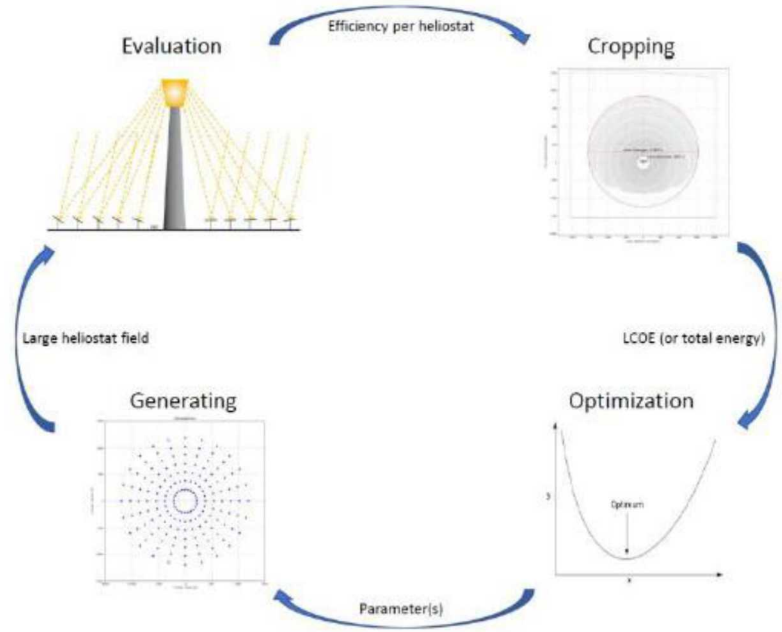

FIGURE 4: basic principle of the heliostat field layout optimization problem.

Simulations and tools developed and showed that introducing a 2^{nd} tower can increase efficiency of heliostat field through receiver switching.
However, LCOE not increased.

CSP System Temperature Range Optimization for Reduced LCOE

Buck and Giuliano, DLR

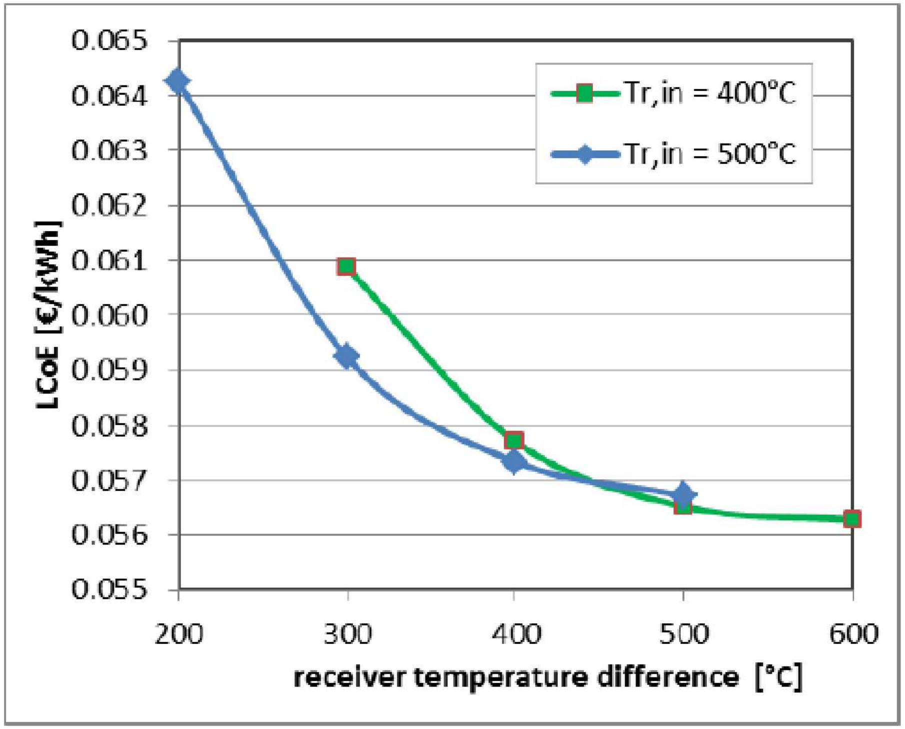

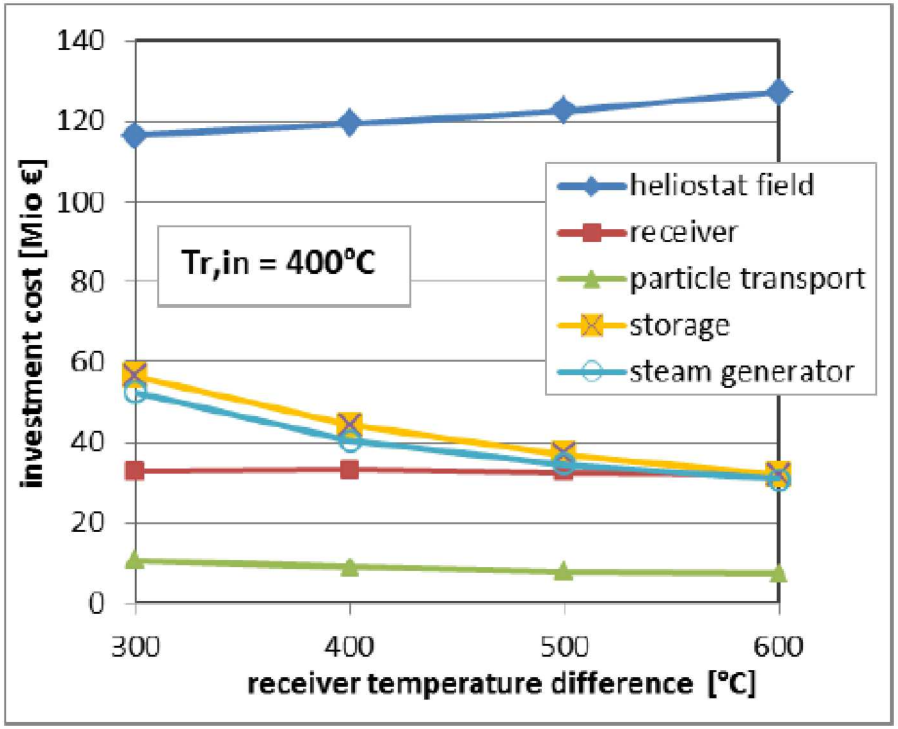

Systems modeling evaluated trade-offs of higher temperatures and ΔT vs. costs of heliostat field, receiver, transport, and LCOE. Results show lower LCOE with higher temperatures and ΔT.

Techno-Economic Assessment of New Material Developments in Central Receiver Solar Power Plants

(Zoshke et al., Fraunhofer ISE and DLR)

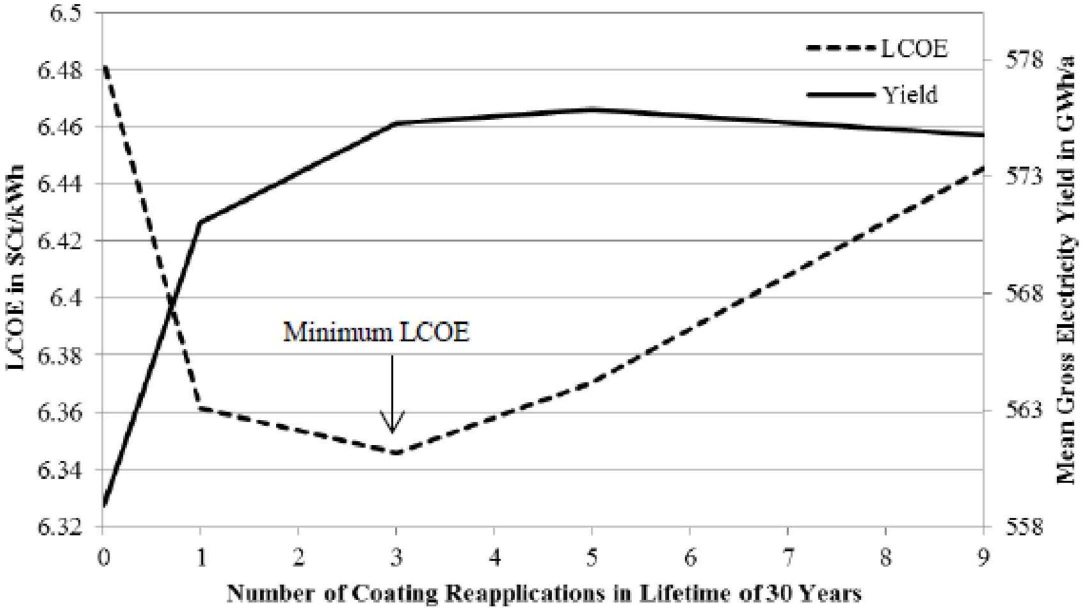

Developed tools to evaluate system behavior every minute of the year *with dynamic degradation of receiver coatings* to assess the optimal reapplication interval and minimum LCOE.

Modeling and measurement of cloud passages

Improved Efficiency Prediction of a Molten Salt Receiver
Based on Dynamic Cloud Passage Simulation, Schwager et al, Aachen University and DLR

Optimization of Robust Aiming Strategies in Solar Tower
Power Plants Considering Clouds and Uncertainties, Richter et al., KIT

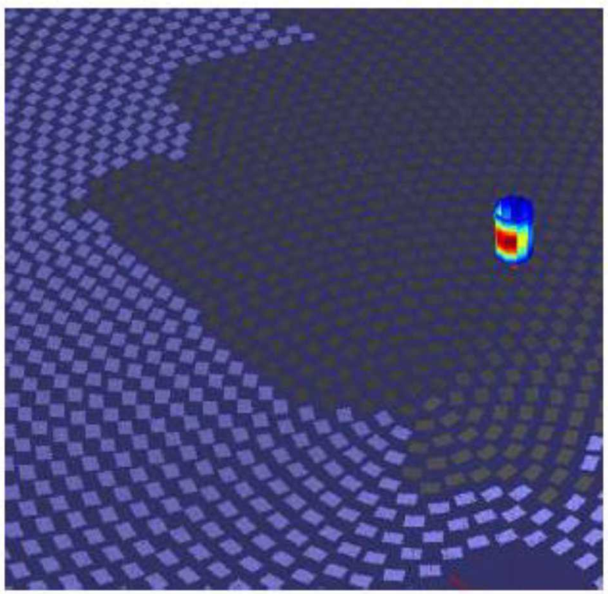

Need distributed DNI measurements

Spatial DNI Measurement for Accurate Solar Flux Control in Megalim 121MWe Solar Receiver Power Plant, Minis et al., BrightSolurce.

Use of PV module on each heliostat to monitor local DNI

Object Oriented Modelling of the CSP-DSW Facility

Corbett et al., Cypress Institute

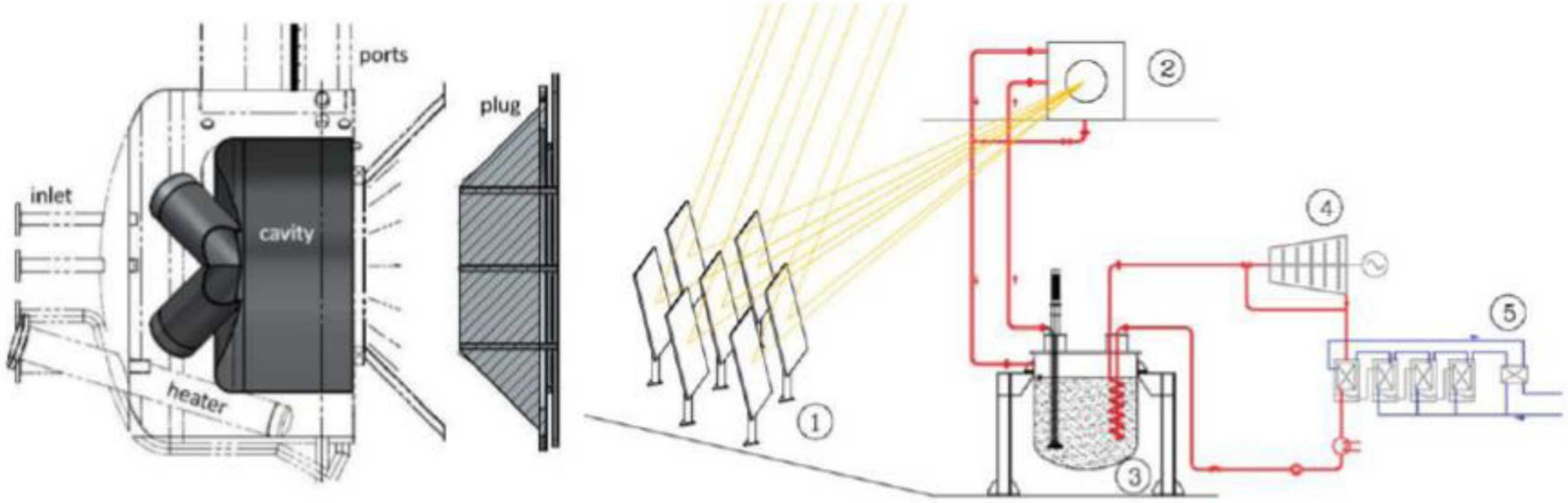

FIGURE 2. Left: ISTORE [8]; Right PROTEAS Operation Schematic: (1) heliostat field; (2) central receiver; (3) molten salt storage tank; (4) steam engine; (5) MED desalination unit [8]

Modelica tools were used to simulate CSP for desalination of sea water. Prototype multi-effect distillation units at Cyprus Institute were used to validate the model.

Point-Focus Systems

- Heliostats, Dish Systems, and Optics
- Receivers
- Systems Modeling

Conclusions

- ~120 point-focus papers submitted
  - 36 on heliostats and optics (30%)
  - 5 on dish systems (4%)
  - 45 on receiver systems (38%)
  - 35 on balance of plant and systems modeling (28%)
- Focus on achieving higher temperatures (>700 C) while mitigating convective and radiative heat losses
  - Novel volumetric heating designs
  - Particle-based systems
- Collector aiming and optics, reliability, system analysis, and efficiency very important

Thank you for your attention!

Point-Focus Systems
A Review of Papers Presented at SolarPACES 2018

Clifford K. Ho and Julius E. Yellowhair
Sandia National Laboratories

Sandia National Laboratories

Backup Slides

On-sun test of a single tube fluidized particle solar receiver: Cristobalite powder as heat transfer fluid

(Lopez et al., PROMES-CNRS)

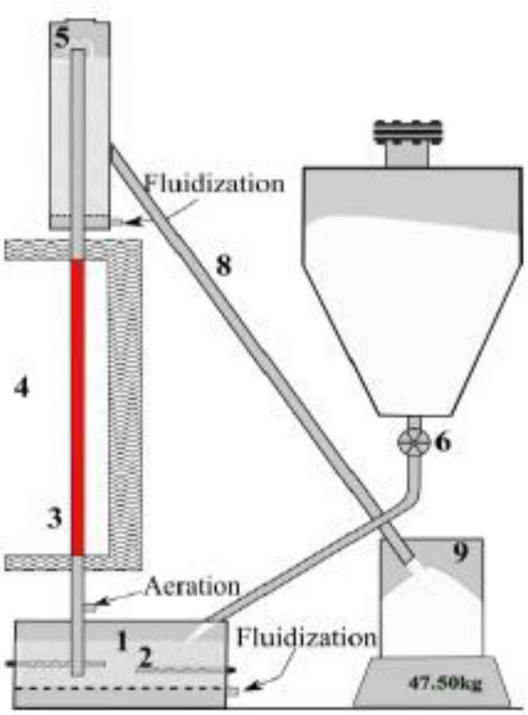

On-sun tests of a dense suspension of Cristobalite powder flowing upward through a tube demonstrated high heating (up to 740 C) at flow rates of 8 – 63 kg/m²/s

Development of High Performance Solar Absorber Coatings

(Harzallah, CMI, Belgium)

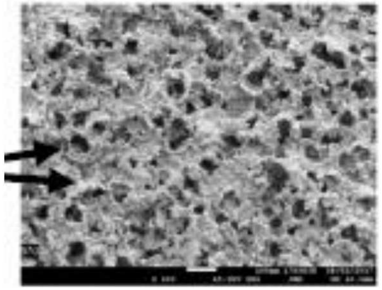

Silicon based absorber coating

Plasma spray absorber coating

Intended for >700 C with 97% absorptance and lower emittance

Particle Heat Exchangers

Integration, Control, and Testing of a High-Temperature Particle-to-sCO2 Heat Exchanger

Albrecht et al., Sandia National Laboratories

Development of View Factor Correlations for Modeling Thermal Radiation in Solid Particle Solar Receivers Using CFD-DEM

(Johnson et al., Middle East Technical University)

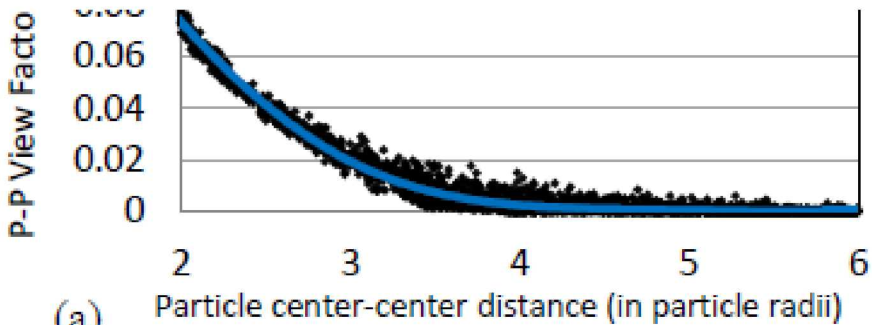

(a)

Development of radiative view factor correlation vs. distance for densely-packed particles to be used in efficient CFD-DEM models